The Effect of Multi-Market Participation on Day-Ahead Trading of an Electricity Producer

Helmi Hankimaa, Fabricio Oliveira
Department of Mathematics and Systems Analysis
Aalto University
Espoo, Finland

Bruno Fanzeres
Industrial Engineering Department
Pontifical Catholic University of Rio de Janeiro
Rio de Janeiro, Brazil

***Abstract*—The operating landscape for electricity producers has changed profoundly as new reserve markets have emerged and intraday trading volumes have increased substantially. Thus, the day-ahead market is no longer the sole focus of generation companies. As multi-market participation becomes widespread and discussions around market design intensify, it is pertinent to understand optimal strategies in this environment, especially how they contrast with traditional day-ahead market-focused strategies. Therefore, we analyse multi-market and day-ahead-focused offer strategies of a hybrid producer. Specifically, offers are optimised for the day-ahead market, the up-regulating frequency containment for the disturbances market, and intraday trading using stochastic programming. We find that up-regulating reserve-market participation reduces day-ahead market participation as expected. However, as this effect only manifests at higher bid prices, this behaviour could be misconstrued as market manipulation. Furthermore, we observe undesirable effects resulting from the model structure that lead to strategies optimising price arbitrage and generating intentional imbalances.**

***Index Terms*—Coordinated Multi-Market Offering, Energy Economics, Hybrid Producers, Nordic Electricity Markets, Stochastic Optimisation**

I. Introduction

The expansion of variable renewable energy (VRE) generation has amplified the need for and the importance of ancillary services [1]. This has fostered the emergence of new reserve markets from where transmission system operators (TSOs) procure resources to maintain grid stability. Additionally, the significant capacity of intermittent generators in the grid has increased the need for post-day-ahead market adjustments, due to which traded volumes in intraday markets have grown [2]. With the opportunities presented by these new reserve markets and more liquidity in intraday markets, the operating field of electricity producers has changed profoundly.

Producers have thus become increasingly interested in participating in multiple markets as opposed to seeing the day-ahead market as the sole short-term revenue stream. However, forming offers for multiple sequentially cleared markets is challenging as the decision-making process involves many uncertainty factors and constraints [3]. Assuming the viewpoint of a price-taker generation company (GenCo), the uncertainties are related to market prices, market liquidity, and VRE generation, and the constraints are associated with the technical operation of generators, market design, and possibly regulation. Moreover, evaluating opportunity costs between temporally separated markets under uncertainty is not straightforward. These challenges motivate the use of offer-strategy optimisation models.

In the literature, numerous models for optimising multi-market offer strategies have been proposed for different contexts and under various assumptions, and many have leveraged a multi-stage stochastic programming framework. Typically, these models are used to evaluate the profitability of participating in certain markets, and a recent direction has also been to evaluate the benefits of coordinating offer strategies across multiple markets as opposed to the traditional practice of optimising offers sequentially. For example, the authors in [4] evaluated the coordination benefits of trading in day-ahead and intraday markets for a Norwegian hydropower plant and concluded the benefits to be negligible at the time. In more recent studies, [5] and [6] also modelled the bidding of Norwegian hydropower producers, focusing however on the day-ahead and balancing markets. Both studies found benefits in participating in the balancing markets with a coordinated approach, even though [6] concluded that using a coordinated strategy is not worthwhile in the current market situation. In addition to the day-ahead and balancing markets, authors in [7] included the frequency containment reserve for normal operation (FCR-N) market in their model and studied whether the coordination benefits were dependent on the portfolio size.

The aforementioned studies are all limited to hydropower, which implies that the generators do not face production uncertainty in the short term. Thus, they do not face a natural risk of imbalances. In contrast, the authors in [8] modelled the optimal self-scheduling of a wind-power producer with inherent uncertainty in production. The context was the Spanish forward, day-ahead, and ancillary markets, and they concluded that participating in multiple markets increases expected profits. In addition to VRE technologies, [9] modelled dispatchable technologies of producers with hybrid portfolios in the Iberian day-ahead, intraday, and balancing markets. They found that considering the intraday markets yielded a significant increase in profits when compared to only participating in the day-ahead and balancing markets. The authors of [10] and [11] also studied coordination benefits, evaluating the value of coordinated offers of a hybrid portfolio as opposed to offering the resources separately. They found that a coordinated offering of a hybrid portfolio is more profitable. Recently, the authors in [12] optimised bids for a hybrid portfolio with VRE and

979-8-3315-1278-1/25/$31.00

dispatchable generators in the day-ahead, intraday and reserve markets in Germany with a focus on the effect of risk-aversion on the optimal trading strategy.

As illustrated above, the offer-strategy optimisation literature mainly focuses on the profitability of different strategies in multi-market settings. However, as the adoption of these multi-market offer strategies for complex hybrid portfolios increases and the discussion around market design intensifies, it is pertinent to understand optimal strategies within this environment, especially how they contrast with traditional day-ahead market-focused ones. In fact, this discussion has been explored by the authors in [6] and [12]. Specifically, the authors in [6] inspected the shifts in day-ahead offer curves when coordinating offers for the day-ahead and balancing markets, contrasting to considering the day-ahead market only. The authors in [12] analysed the optimal positions of a GenCo in a day-ahead, intraday, and reserve market setting, evaluating how the profit distributions across different markets change when different risk preferences are considered.

Our work contributes to the discussion on the effects of multi-market participation on the day-ahead offer strategies of a GenCo owning a hybrid portfolio comprising dispatchable and VRE generators. Methodologically, we devise a stochastic programming model to analyse the effects of multi-market participation by assessing optimal day-ahead offer curves of the hybrid producer in the day-ahead, intraday, and up-regulating frequency containment reserve for disturbances (FCR-D) markets. We assume that the participant does not act in balancing markets but incurs imbalance settlement costs if their generation deviates from market commitments. Our analysis and discussion provide insights into how the inherent decision of withholding capacity from the day-ahead market in favour of participating in the reserve market could be misinterpreted as market manipulation, as well as the impact of the challenges in modelling the imbalance stage may inadvertently lead to illegal trading behaviour.

II. Offer-Strategy Optimisation Model

This section presents an offer-strategy optimisation model for a price-taker GenCo with a hybrid power production portfolio comprising wind turbines, hydropower, and combined cycle gas turbine (CCGT) generators.

A. Market Structure

The GenCo considered in this work participates in the day-ahead, intraday, and the Finnish up-regulating FCR-D markets. The day-ahead market is organised daily for the 24 hours of the following day and cleared at noon with a uniform market-clearing price. Producers submit pairwise-linked price-quantity offers, and the linear interpolation of these price steps forms an offer curve. Intraday trading occurs after the day-ahead market is cleared on markets with continuous matching and three intraday auctions. The Finnish TSO organises a market for up-regulating FCR-D for all delivery hours of the following day. This market closes at 17:30 CET [13]. The offers to the market consist of capacity-price pairs. A producer may submit multiple offers, which are processed separately and, hence, effectively form an increasing step curve. Although the Nordic TSOs currently use a one-price imbalance settlement system, in this work, we model the two-price imbalance settlement system that was in place until November 2021. The two-price imbalance settlement system is outlined in [14].

B. Scenario Structure

The model incorporates two decision stages. In the first stage, the day-before-delivery decisions are optimised. These include optimising offers for the day-ahead and up-regulating FCR-D markets. The second stage comprises the day-of-delivery decisions. These include the possibility of the GenCo submitting one buy or sell order per delivery hour to the intraday markets. In reality, GenCos are able to make several orders in intraday markets, but this restriction was made to contain the complexity of the model. In addition to intraday trades, the production planning of the GenCo's units is modelled in the second stage. Uncertainty is modelled using a scenario tree, where each node in the tree comprises values for all 24 delivery hours. After the first-stage decisions, the day-ahead and up-regulating FCR-D market prices are observed, and commitments to both markets are determined for each price scenario $s \in \mathcal{S}$. Each scenario $s \in \mathcal{S}$ corresponds to a set of intraday market price scenarios, $\mathcal{E}$. Second-stage decisions are modelled for each scenario $e \in \mathcal{E}$. The leaf nodes of the scenario tree correspond to the real-time realisations of wind availability and balancing prices, $\omega \in \Omega$. Due to the observation of wind availability, this is also the stage where the imbalances of the GenCo are determined. An illustration of the scenario tree is provided in the Appendix.

C. Profit-Maximising Objective Function

The objective function maximises the expected profit from the strategy over all delivery hours $t \in \mathcal{T}$ for a single day. More specifically, it is defined as

$$\sum_{t\in\mathcal{T}}\sum_{s\in\mathcal{S}} \pi_s^S \left(\rho_{ts} y_{ts} + \psi_{ts} r_{ts} + \sum_{e\in\mathcal{E}} \pi_e^E \varphi_{tse} z_{tse} \right) \tag{1a}$$

$$- \sum_{t\in\mathcal{T}}\sum_{s\in\mathcal{S}}\sum_{e\in\mathcal{E}} \pi_s^S \pi_e^E \Big(S^{H,start} u_{tse}^{H,start} \tag{1b}$$

$$+ S^{C,gen} g_{tse}^{C} + S^{C,start} u_{tse}^{C,start} + S^{C,stop} u_{tse}^{C,stop} \Big) \tag{1c}$$

$$+ \sum_{s\in\mathcal{S}}\sum_{e\in\mathcal{E}} \pi_s^S \pi_e^E \Big(V(l_0) - V(l_{T,se}) \Big) \tag{1d}$$

$$+ \sum_{t\in\mathcal{T}}\sum_{s\in\mathcal{S}}\sum_{e\in\mathcal{E}}\sum_{\omega\in\Omega} \pi_s^S \pi_e^E \pi_\omega^\Omega \Big(\lambda_{tse\omega}^{+} \Delta_{tse\omega}^{+} - \lambda_{tse\omega}^{-} \Delta_{tse\omega}^{-} \Big). \tag{1e}$$

In the objective function (1), π^S, π^E and π^Ω denote probabilities defined over the scenario sets $\mathcal{S}, \mathcal{E}$ and Ω, respectively. Terms (1a) capture revenue from day-ahead market commitments y_{ts} sold at prices ρ_{ts}, revenue from capacity fees ψ_{ts} received for reserved capacity r_{ts} and revenue or costs from trades z_{tse} in the intraday markets at prices φ_{tse}. Terms (1b) and (1c) capture the production costs incurred from the start-up of the hydropower generator and costs from running, starting

up and shutting down the CCGT. The superscripts of the cost parameters differentiate the specific costs. Letters H and C denote the hydropower and CCGT generators, respectively. Binary variables u_{tse}, u_{tse}^{start} and u_{tse}^{stop} represent the on-off state, start-up, and shutdown of units. Terms (1d) denote the opportunity cost associated with hydropower generation, modelled using a future water value function (shown in the Appendix), analogous to [15]. The value of water level l in the reservoir is given by the water value function $V(l)$, with l_0 denoting initial water levels and $l_{T,se}$ standing for final water levels in scenario $(s, e) \in (\mathcal{S}, \mathcal{E})$. Finally, terms (1e) capture the revenue from the imbalance settlement. In a two-price imbalance settlement system, the GenCo receives the down-regulation price $\lambda_{tse\omega}^{+}$ for excess energy and is charged the up-regulation price $\lambda_{tse\omega}^{-}$ for deficits. Depending on the system state, one of these prices is always equal to the day-ahead price, and the inequality $\lambda_{tse\omega}^{+} \leq \rho_{ts} \leq \lambda_{tse\omega}^{-}$ holds for all hours $t \in \mathcal{T}$ and scenarios $s \in \mathcal{S}$. The positive and negative imbalances of the GenCo for each hour $t \in \mathcal{T}$ are denoted by nonnegative variables $\Delta_{tse\omega}^{+}$ and $\Delta_{tse\omega}^{-}$, respectively.

D. Offering and Imbalance Constraints

The day-ahead offer curve is formulated according to [15] with I price steps. To avoid a non-linear formulation, the prices p_i for each offer $i \in \mathcal{I}$ are fixed. These prices are ordered such that $p_i < p_{i+1}$ for all $i \in \mathcal{I} \setminus I$. The offer quantities are denoted by nonnegative continuous variables x_{it} for all $i \in \mathcal{I}, t \in \mathcal{T}$, that capture the total quantity offered at prices up to p_i. Since the market regulations require that the offer curve must be increasing, the following constraint is imposed on these variables:

$$x_{it} \leq x_{i+1,t} \quad \forall i \in \mathcal{I} \setminus \{I\}, t \in \mathcal{T}. \tag{2}$$

The day-ahead market commitment for each hour $t \in \mathcal{T}$ and scenario $s \in \mathcal{S}$ is derived using the market-clearing price ρ_{ts}. The commitment is determined by the intersection of the offer curve and the market price, given as

$$y_{ts} = \begin{cases} \frac{\rho_{ts}-p_1}{p_2-p_1} x_{2t} + \frac{p_2-\rho_{ts}}{p_2-p_1} x_{1t}, & \text{if } p_1 \leq \rho_{ts} < p_2 \\ \quad \vdots & \\ \frac{\rho_{ts}-p_i}{p_{i+1}-p_i} x_{i+1,t} + \frac{p_{i+1}-\rho_{ts}}{p_{i+1}-p_i} x_{it}, & \text{if } p_i \leq \rho_{ts} < p_{i+1} \\ \quad \vdots & \\ \frac{\rho_{ts}-p_{I-1}}{p_I-p_{I-1}} x_{It} + \frac{p_I-\rho_{ts}}{p_I-p_{I-1}} x_{I-1,t}, & \text{if } p_{I-1} \leq \rho_{ts} < p_I. \end{cases} \tag{3}$$

The GenCo submits J up-regulating capacity offers to the reserve market. The offer quantities are denoted by v_{jt} for all $j \in \mathcal{J}, t \in \mathcal{T}$ and the corresponding prices are ordered such that $p_j < p_{j+1}$ for all $j \in \mathcal{J} \setminus J$. The committed reserve capacity r_{ts} is the sum of all cleared offers for hour t in scenario s, i.e.,

$$r_{ts} = \begin{cases} 0, & \text{if } \psi_{ts} \leq p_1 \\ v_{1t}, & \text{if } p_1 \leq \psi_{ts} \leq p_2 \\ v_{1t} + v_{2t}, & \text{if } p_2 \leq \psi_{ts} \leq p_3 \\ \quad \vdots & \\ v_{1t} + v_{2t} + \cdots + v_{Jt}, & \text{if } p_J \leq \psi_{ts}. \end{cases} \tag{4}$$

Furthermore, the GenCo cannot bid more than its generation capacity, which is given as the sum of its CCGT, hydro and wind capacities: C^C, C^H and C^W. This is imposed as

$$x_{It} + \sum_{j \in J} v_{jt} dt \leq (C^C + C^H + C^W) dt \qquad \forall t \in \mathcal{T}, \tag{5}$$

where the one-hour time interval, dt, is used for the power-energy conversion. Moreover, the GenCo cannot generate and reserve more than its capacity. Therefore,

$$y_{ts} + r_{ts} dt \leq (C^C + C^H + C^W) dt \quad \forall t \in \mathcal{T}, s \in \mathcal{S}, e \in \mathcal{E}. \tag{6}$$

Reserve commitments must be fulfilled by the hydropower and CCGT generators. Thus,

$$r_{ts} = r_{tse}^{H} + r_{tse}^{C} \quad \forall t \in \mathcal{T}, s \in \mathcal{S}, e \in \mathcal{E}, \tag{7}$$

where variables r_{tse}^{H} and r_{tse}^{C} denote reserve capacity provided by the hydropower and CCGT generators, respectively.

Intraday trades are denoted by real-valued variables z_{tse}. A positive value of z_{tse} represents selling energy and a negative value represents buying energy. Similarly as was done in [4] and [12], a limit on intraday trading is imposed. The limit is specified as a percentage, α, of the total installed capacity of the GenCo as in (8).

$$\mid z_{tse} \mid \leq \alpha (C^C + C^H + C^W) dt \quad \forall t \in \mathcal{T}, s \in \mathcal{S}, e \in \mathcal{E}. \tag{8}$$

Along with day-ahead and reserve commitments, intraday trading cannot exceed the maximum generation capacity in any scenario. Therefore,

$$y_{ts} + r_{ts} dt + z_{tse} \leq (C^C + C^H + C^W) dt \quad \forall t \in \mathcal{T}, s \in \mathcal{S}, e \in \mathcal{E}. \tag{9}$$

The generation company's imbalance is defined as

$$\Delta_{tse\omega}^{+} - \Delta_{tse\omega}^{-} = g_{tse}^{C} + g_{tse}^{H} + g_{tse\omega}^{W} - (y_{ts} + z_{tse}) \quad \forall t \in \mathcal{T}, s \in \mathcal{S}, e \in \mathcal{E}, \omega \in \Omega, \tag{10}$$

where g_{tse}^{C}, g_{tse}^{H} and $g_{tse\omega}^{W}$ denote the real-time generation of the CCGT, hydropower and wind-powered generators, respectively. The restriction of only one of the imbalance variables being non-zero at a time is handled in a post-optimisation procedure, described in the Appendix. The procedure finds the optimal solution with the least imbalances out of possible degenerate solutions. Furthermore, valid inequalities (shown in the Appendix) are introduced to bound imbalances according to [16].

E. Operational constraints

The constraints characterising the operation of the hydropower, CCGT, and wind units are included in the Appendix. The hydropower, CCGT generator, and wind power constraints are adapted from [15], [17] and [18], and [16], respectively. The hydropower and CCGT generators are dispatchable units, but the wind power output is uncertain. The wind unit has a maximum generation level modelled using a capacity factor over the installed capacity. The capacity factor encodes the exogenous uncertainty related to wind availability, and thus, multiple scenarios are considered for this parameter.

III. Numerical Analysis

In our numerical analysis, the model is optimised using a scenario tree comprising 180 scenarios. Ten day-ahead and reserve prices were chosen from historical data from years 2022 and 2023 based on covariate information, such as temporal and market-setting information so that they are representative of winter-season weekdays. Six intraday prices were sampled from these chosen days, and distributions with three values for wind and balancing price realisations were generated around their true values. The historical data was retrieved from the ENTSO-E Transparency Platform [19], Fingrid's open data sets [20]–[22], and intraday trading data was received from Nord Pool.

Production parameters were chosen such that the GenCo's portfolio comprises a 170 MW CCGT unit, a 100.8 MW hydropower unit, and 40 MW of wind power. The startup and shutdown costs of the generators are assumed to be negligible, and the water value function is modelled as a single linear function. We consider 34 price steps for the day-ahead offer curve and 17 price steps for the reserve offer curve, chosen such that they cover a plausible price range.

The model was implemented using JuMP [23] in Julia and solved using Gurobi 11.0.2. The experiments were run on a MacBook Air with an Apple M3 chip and 16 GB of memory.

A. Effects of Reserve Market Participation

To evaluate the effects of a multi-market strategy on day-ahead offers, we analysed three experimental set-ups:

(1) **Day-ahead market only**: Optimising the model with only the day-ahead market.
(2) **Day-ahead and reserve markets coordinated**: Optimising day-ahead and up-regulating FCR-D offers.
(3) **All markets coordinated**: Optimising decision-making in all three markets in a coordinated manner.

Fig. 1 displays the day-ahead offer curves of strategies (1), (2) and (3) for a representative hour and exposes interesting effects of coordinated offers for multiple markets. The day-ahead offer curve from strategy (1) functions as the base case, representing traditional day-ahead focused bidding. We notice that strategies (2) and (3) withhold capacity compared to strategy (1) as expected since part of the capacity is allocated to the reserve market. However, perhaps unintuitively, the capacity is only withheld in scarcity situations, reflected by high prices. This behaviour may be misconstrued as price manipulation. However, in this case, it is explained by the GenCo's co-optimisation of the day-ahead and reserve market offers. Pricing according to opportunity costs in sequentially cleared markets is acceptable in the REMIT regulation [24]. Therefore, despite the resemblance to market manipulation, scrutiny from a regulatory authority would be unwarranted in this case. The authors in [6] observed a similar effect when coordinating offers for the day-ahead and balancing markets. They also observed the reverse effect when considering a down-regulating reserve market: the optimal strategy was to oversupply at low prices.

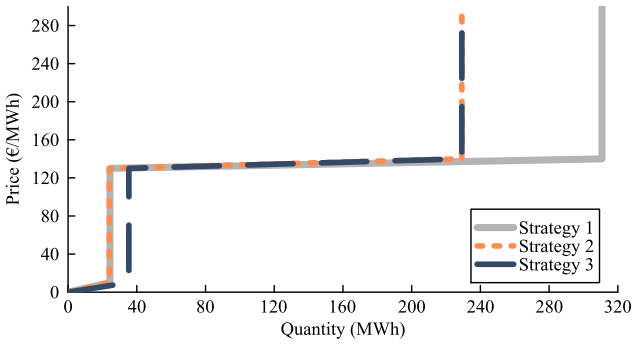

Fig. 1. Day-ahead offer curves with strategies (1), (2) and (3).

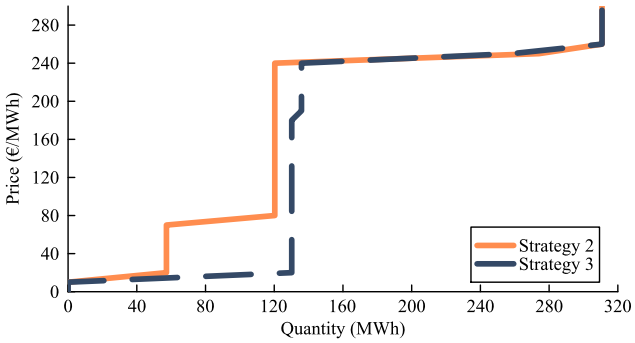

Fig. 2. Day-ahead offer curves with strategies (2) and (3).

B. Effects of Intraday Trading and Imbalance Settlement

Fig. 2 shows optimal offer curves from strategies (2) and (3) for a selected representative hour. We observe that, in strategy (3), the offer curve is shifted to the right compared to strategy (2), indicating that a larger capacity is offered at lower prices. The shift is due to expectations regarding price premiums between the day-ahead and intraday market: in this particular hour, the expected intraday prices are lower than the expected day-ahead price. Thus, strategy (3) oversells in the day-ahead market and plans to buy part of their commitments in the intraday market, in effect doing price arbitrage. Price arbitrage is not illegal unless the extent of it is such that it has an effect on market prices. This observation illustrates the significance of constraint (8) in the model because it limits the capacity that can be used for price arbitrage. However, we recognise that a GenCo's risk preferences may naturally steer them away from betting on intraday markets, as shown in [12].

Note that, for this numerical analysis, intraday trades were capped at 15 MW per hour by setting $\alpha = 0.05$ in (8). However, from Fig. 2, we notice a larger (higher than 15 MW) shift in the lower section of the offer curve. This shift is partially explained by the fact that, in this particular hour, the expected balancing prices reflected a down-regulation period. Thus, the optimal (anticipated) strategy in this hour is to oversell in the day-ahead market and make a profit from a generation deficit. We observe this behaviour in all strategies; however, the expected imbalances of the GenCo

were largest using strategy (3). This is because in strategy (3), intraday trading is used to increase price arbitrage with respect to balancing prices. This occurs because, in a multi-stage stochastic program, second-stage decisions (including intraday trades) are made with more information on the balancing prices, which are revealed in the leaf nodes of the scenario tree. The opposite effects were found in hours where the expected balancing prices reflected an up-regulation period.

Submitting an offer curve to the day-ahead market with the intent of generating an imbalance violates Nordic balance agreements. This could also be seen to give a misleading signal of available supply, which is illegal under REMIT. Moreover, this price arbitrage strategy leaves the GenCo exposed to greater price risks in the imbalance-settlement stage. Note that the modelled GenCo does not participate in the balancing markets. Thus, since the offer strategies purposefully over- and under-bid in an effort to perform price arbitrage, these optimal offers are unsuitable for real-world implementation.

We must highlight that some studies attempt to mitigate this behaviour by introducing constraints and penalties for imbalances. Studies such as [4] and [6] model dispatchable generators and constrain expected imbalances to be zero with a constraint of the form

$$\sum_{s\in\mathcal{S},e\in\mathcal{E},\omega\in\Omega} (\Delta^{+}_{tse\omega} - \Delta^{-}_{tse\omega}) = 0 \quad \forall t \in \mathcal{T}. \tag{11}$$

Note that this constraint may be unsuitable for portfolios with VRE generators due to inherent uncertainty in output.

Another approach, taken in [12], where a hybrid portfolio of dispatchable and VRE generators is modelled, replaces the imbalance settlement terms in the objective and penalises all imbalances with a penalty:

$$penalty \;=\; \sum_{t\in\mathcal{T},s\in\mathcal{S},e\in\mathcal{E},\omega\in\Omega} \Lambda(\Delta^{+}_{tse\omega} + \Delta^{-}_{tse\omega}). \tag{12}$$

Fig. 3 illustrates day-ahead offer curves of strategy (2), strategy (3), two novel versions of strategy (3): one with constraint (11) and one where all imbalances are penalised according to (12) for an expected up-regulation hour. For expository purposes, the penalty price Λ was set to be higher than all day-ahead price values in the scenario set. The offer curves in Fig. 3 demonstrate that the way imbalances are modelled significantly affects the optimal strategies, and that introducing constraint (11) or penalties according to (12) both steer the model not to under-bid in an expected up-regulation hour. The model with the penalty offers the most capacity at mid-range prices in this case. Out of these models, the expected imbalances are the smallest with constraint (11) as it sets them to zero. However, the total expected excess and deficit generation $\sum_{s\in\mathcal{S},e\in\mathcal{E},\omega\in\Omega} \pi_s\pi_e\pi_w(\Delta^{+}_{tse\omega} + \Delta^{-}_{tse\omega})$ for hours $t \in \mathcal{T}$ are the smallest, in fact near zero, when all imbalances are penalised. Notably, in the other models, the total expected deviations are approximately 100 times larger. Thus, the strategy where all imbalances are penalised would be the most straightforward to justify in light of regulations. Furthermore, the small expected imbalances leave the GenCo significantly less exposed to risks associated with balancing price fluctuations.

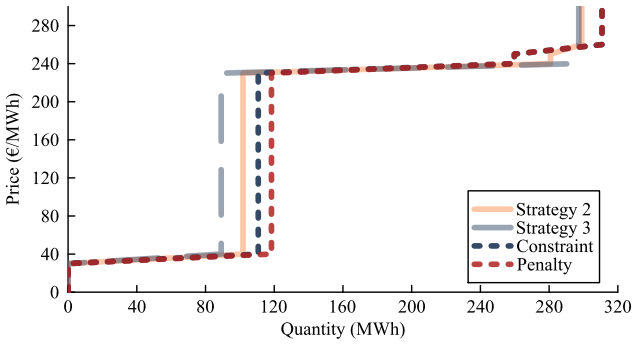

Fig. 3. Offer curves for the day-ahead market with strategies (2) and (3) with multiple approaches to imbalances.

IV. Conclusion

Our work analyses the use of a stochastic programming model for optimising a multi-market offer strategy for day-ahead, intraday, and up-regulating FCR-D trading in the European, specifically Finnish, context. Our contribution is that we assess how coordinating offers in a multi-market setting affects day-ahead trading and how these optimal strategies align with regulations. The effects were analysed by inspecting day-ahead offer curves. It was found that participating in an up-regulating reserve market resulted in withheld capacity from the day-ahead market at high prices, which resembles behaviour attempting to manipulate the market.

Furthermore, we observed that this model structure finds strategies that optimise price arbitrage, even planning intentional generation imbalances to leverage imbalance settlement prices. Deliberately planning generation imbalances violates market agreements. Moreover, while price arbitrage is not illegal, these strategies expose the producer to greater price risk in the post-day-ahead markets. We note that similar effects are likely to be observed if a one-price imbalance settlement system is modelled instead.

A limitation of our study is that we did not assess what the actual imbalances would be if the explored strategies were implemented, as a multi-stage model does not determine optimal decisions for second-stage decisions. Additionally, the profitability levels of the strategies were not assessed. These are questions left for further research. Furthermore, follow-on research might evaluate the system-wide implications as multi-market strategies become more prevalent among participants, in contrast to day-ahead market-focused strategies.

Acknowledgment

Helmi Hankimaa and Fabricio Oliveira gratefully acknowledge the support from the Research Council of Finland (decision number 348092). Bruno Fanzeres gratefully acknowledges the support from CAPES (Finance Code 001), CNPq (project 309064/2021-0), and FAPERJ (project E-26/204.553/2024).

References

[1] J. Katz, P. Denholm, and J. Cochran, "Balancing area coordination: Efficiently integrating renewable energy into the grid, greening the grid," 2015. [Online]. Available: https://www.nrel.gov/docs/fy15osti/63037.pdf

[2] I. Z. Stuart Disbrey, "Nord pool reports encouraging growth in 2024," Nord Pool AS, Lysaker, Norway. Published: 22.1.2025. [Online].

[3] R. Scharff, J. Egerer, and L. Söder, "A description of the operative decision-making process of a power generating company on the nordic electricity market," *Energy Systems*, vol. 5, pp. 349–369, 2014.

[4] E. Faria and S.-E. Fleten, "Day-ahead market bidding for a nordic hydropower producer: taking the elbas market into account," *Computational Management Science*, vol. 8, pp. 75–101, 2011.

[5] E. K. Aasgård, "The value of coordinated hydropower bidding in the nordic day-ahead and balancing market," *Energy Systems*, vol. 13, no. 1, pp. 53–77, 2022.

[6] G. Klæboe, J. Braathen, A. L. Eriksrud, and S.-E. Fleten, "Day-ahead market bidding taking the balancing power market into account," *Top*, vol. 30, no. 3, pp. 683–703, 2022.

[7] H. Kongelf, K. Overrein, G. Klæboe, and S.-E. Fleten, "Portfolio size's effects on gains from coordinated bidding in electricity markets: A case study of a norwegian hydropower producer," *Energy Systems*, vol. 10, pp. 567–591, 2019.

[8] M. Shafie-khah, A. S. de la Nieta, J. Catalão, and E. Heydarian-Forushani, "Optimal self-scheduling of a wind power producer in energy and ancillary services markets using a multi-stage stochastic programming," in *2014 Smart Grid Conference (SGC)*. IEEE, 2014, pp. 1–5.

[9] A. R. Silva, H. Pousinho, and A. Estanqueiro, "A multistage stochastic approach for the optimal bidding of variable renewable energy in the day-ahead, intraday and balancing markets," *Energy*, vol. 258, p. 124856, 2022.

[10] H. Khaloie, A. Abdollahi, M. Shafie-Khah, P. Siano, S. Nojavan, A. Anvari-Moghaddam, and J. P. Catalão, "Co-optimized bidding strategy of an integrated wind-thermal-photovoltaic system in deregulated electricity market under uncertainties," *Journal of Cleaner Production*, vol. 242, p. 118434, 2020.

[11] H. Khaloie, A. Anvari-Moghaddam, J. Contreras, J.-F. Toubeau, P. Siano, and F. Vallée, "Offering and bidding for a wind producer paired with battery and caes units considering battery degradation," *International Journal of Electrical Power & Energy Systems*, vol. 136, p. 107685, 2022.

[12] E. Kraft, M. Russo, D. Keles, and V. Bertsch, "Stochastic optimization of trading strategies in sequential electricity markets," *European Journal of Operational Research*, vol. 308, no. 1, pp. 400–421, 2023.

[13] "Appendix 1 to the yearly market agreement and hourly market agreement of frequency containment reserves unofficial translation terms and conditions for providers of frequency containment reserves (fcr)," Fingrid Oyj, Tech. Rep., November 2021.

[14] A. Skajaa, K. Edlund, and J. M. Morales, "Intraday trading of wind energy," *IEEE Transactions on power systems*, vol. 30, no. 6, pp. 3181–3189, 2015.

[15] S.-E. Fleten and T. K. Kristoffersen, "Stochastic programming for optimizing bidding strategies of a nordic hydropower producer," *European Journal of Operational Research*, vol. 181, no. 2, pp. 916–928, 2007.

[16] A. J. Conejo, M. Carrión, J. M. Morales *et al.*, *Decision making under uncertainty in electricity markets*. Springer, 2010, vol. 1.

[17] H. Khaloie, A. Abdollahi, M. Shafie-Khah, A. Anvari-Moghaddam, S. Nojavan, P. Siano, and J. P. Catalão, "Coordinated wind-thermal-energy storage offering strategy in energy and spinning reserve markets using a multi-stage model," *Applied Energy*, vol. 259, p. 114168, 2020.

[18] E. Pursiheimo, D. Sundell, J. Kiviluoma, and H. Hankimaa, "Predicer: abstract stochastic optimisation model framework for multi-market operation," *Optimization and Engineering*, pp. 1–30, 2023.

[19] "Day-ahead prices," ENTSO-E Transparency Platform. Accessed: 2.5.2023. [Online].

[20] "Frequency containment reserves for disturbances upwards regulation, hourly market prices," Fingrid Oyj. Accessed: 2.5.2023. [Online].

[21] "Wind power generation forecast - updated once a day," Fingrid Oyj. Accessed: 2.5.2023. [Online].

[22] "Total production capacity used in the wind power forecast," Fingrid Oyj. Accessed: 2.5.2023. [Online].

[23] M. Lubin, O. Dowson, J. Dias Garcia, J. Huchette, B. Legat, and J. P. Vielma, "JuMP 1.0: Recent improvements to a modeling language for mathematical optimization," *Mathematical Programming Computation*, 2023.

[24] European Commission, Regulation (EU) 2024/1106 of the European Parliament and of the Council of 11 April 2024 amending Regulations (EU) No 1227/2011 and (EU) 2019/942 as regards improving the Union's protection against market manipulation on the wholesale energy market, April 2024.

Appendix

A. Scenario Tree

Fig. 4 shows an illustrative scenario tree. The illustrated scenario tree comprises two values for day-ahead and up-regulating FCR-D prices, denoted by $s \in \mathcal{S}$. Followed by two intraday prices per first-stage price realisation, denoted by $e \in \mathcal{E}$, and three values for wind and balancing price realisations per second-stage price realisation, denoted by $\omega \in \Omega$. Therefore, the illustrated scenario tree comprises 12 scenarios.

In the numerical experiment, we considered ten values for day-ahead and up-regulating FCR-D prices, then six intraday prices for each of these scenarios, and finally, three values for wind and balancing price realisations per price scenario. Therefore, the scenario tree that we modelled comprised $10 \times 6 \times 3 = 180$ scenarios in total.

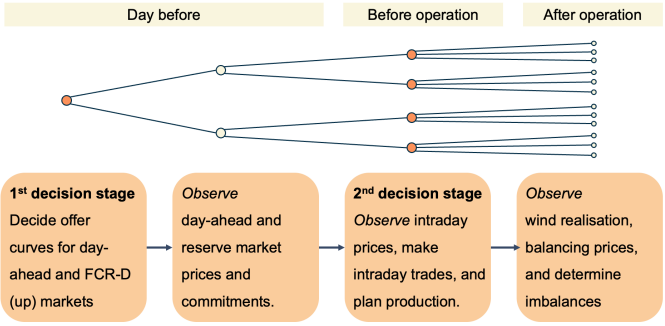

Fig. 4. Illustration of scenario tree.

B. Water Value Function

The water value function is used to calculate the value of the water stored in the reservoir. It is approximated by a piecewise linear function, defined as

$$V(l_t) = \min_{k \in \mathcal{K}} \{B_1^k l_t + B_2^k\}, \tag{13}$$

where B_1^k and B_2^k are coefficients of the linear functions $k \in \mathcal{K}$ that constitute the concave piecewise linear function, and l_t represents the water level in the reservoir at time t.

C. Post-Optimisation Procedure

The model may yield many optimal, degenerated solutions. The degeneracy arises due to modelling the two-price imbalance settlement system, where at least one of the up- or down-regulation prices, λ^- or λ^+, is equal to the day-ahead market price. Thus, in some scenarios, the model may be

indifferent between allocating energy to the day-ahead market or generating an imbalance, if it receives the day-ahead price for the imbalance. In these cases, the optimal solution may have non-zero excess and deficit generation in a delivery hour, such that both $\Delta^+, \Delta^- > 0$. For these degenerate solutions there always exists an alternative optimal solution where the difference between Δ^+ and Δ^- is the same but only one of the imbalances is non-zero. In the alternative optimal solution, the quantity of energy that is reduced from both imbalances to make one of them zero is allocated to the day-ahead market. To deal with degeneracy and to ensure that only one of the imbalances (Δ^+ or Δ^-) can be positive at a time, we utilise a post-optimisation procedure that finds the optimal solution with the least imbalances.

In the post-optimisation procedure, once the optimisation model is solved and the objective value is found, a constraint enforcing that the objective function is equal to this objective value is added to the model. The objective is seen in Equation (1a)–(1e), and we denote it in this section with $\Pi(y, r, z, u^{H,start}, u^C, u^{C,start}, u^{C,stop}, l, \Delta^+, \Delta^-)$. To prevent any unwanted numerical issues, this requirement can be alternatively represented as

$$\Pi(y, r, z, u^{H,start}, u^C, u^{C,start}, u^{C,stop}, l, \Delta^+, \Delta^-) \geq \text{objective value} - \epsilon, \tag{14}$$

where ϵ is a small positive value. After this constraint is added, the objective is changed so that imbalances are minimised. Thus, the formulation of the optimisation problem is

$$\min \quad \sum_{t\in\mathcal{T}}\sum_{s\in\mathcal{S}}\sum_{e\in\mathcal{E}}\sum_{\omega\in\Omega}\left(\Delta^+_{tse\omega} + \Delta^-_{tse\omega}\right)$$
$$\text{s.t.} \quad (2)\text{–}(10),\ (14),\ (15)\text{–}(38).$$

This optimisation finds the optimal offer strategy that attains the highest expected profit with minimal imbalances. This is because constraint (14) ensures that the maximum expected profit level found by the first optimisation model is not compromised.

D. Valid Inequalities for Imbalances

Valid inequalities are formulated to form upper bounds on the positive and negative deviations to get a tighter formulation, thereby improving computational performance. These constraints are adapted from [16]. The upper bounds are stated as

$$\Delta^+_{tse\omega} \leq (C^C + C^H)dt + g^W_{tse\omega}\ \forall t \in \mathcal{T}, s \in \mathcal{S}, e \in \mathcal{E}, \omega \in \Omega, \tag{15}$$

$$\Delta^-_{tse\omega} \leq (C^C + C^H + C^W)dt\ \forall t \in \mathcal{T}, s \in \mathcal{S}, e \in \mathcal{E}, \omega \in \Omega. \tag{16}$$

E. Short-Term Hydropower Production

The hydropower generator model is adapted from [15] and is defined as follows:

$$u^H_{tse} = u^H_{t-1,se} + u^{H,start}_{tse} - u^{H,stop}_{tse} \quad \forall t \in \mathcal{T}, s \in \mathcal{S}, e \in \mathcal{E} \tag{17}$$
$$u^H_{tse} \geq u^{H,start}_{tse} \quad \forall t \in \mathcal{T}, s \in \mathcal{S}, e \in \mathcal{E} \tag{18}$$
$$u^H_{tse} \leq 1 - u^{H,stop}_{tse} \quad \forall t \in \mathcal{T}, s \in \mathcal{S}, e \in \mathcal{E} \tag{19}$$
$$u^H_0 = U^H_{init} \tag{20}$$
$$g^H_{tse} = \eta f_{tse} dt \quad \forall t \in \mathcal{T}, s \in \mathcal{S}, e \in \mathcal{E} \tag{21}$$
$$f_{tse} + r^H_{tse}/\eta \leq u^H_{tse} F^{max} \quad \forall t \in \mathcal{T}, s \in \mathcal{S}, e \in \mathcal{E} \tag{22}$$
$$u^H_{tse} F^{min} \leq f_{tse} \quad \forall t \in \mathcal{T}, s \in \mathcal{S}, e \in \mathcal{E} \tag{23}$$
$$L^{min} \leq l_{tse} \leq L^{max} \quad \forall t \in \mathcal{T}, s \in \mathcal{S}, e \in \mathcal{E} \tag{24}$$
$$l_0 = L^{init} \tag{25}$$
$$l_{tse} = l_{t-1,se} - f_{tse} - f^{spill}_{tse} + F^{in}_t dt\ \forall t \in \mathcal{T}, s \in \mathcal{S}, e \in \mathcal{E}. \tag{26}$$

Constraints (17)–(19) capture whether the hydropower generator is turned on or off and restrict it to be either on or off at each time $t \in \mathcal{T}$ in each scenario $(s, e) \in (\mathcal{S}, \mathcal{E})$. Constraint (20) sets the generator's initial state to $U^H_{init} \in \{0, 1\}$. Discharging water generates energy, which is modelled in (21). Coefficient η captures the relationship between the rate of discharge, f_{tse}, and power, and accounts for the efficiency of the generator. Constraints (22) and (23) define bounds for the rate of discharge, f_{tse}. The minimum and maximum discharge capacities are denoted by F^{min} and F^{max}. Note that the reserved capacity is assumed not to be activated. Thus, the reserve provided by hydropower, r^H_{tse}, is only accounted for in the upper bound for the rate of discharge. Constraint (24) defines the limits for the water level in the reservoir, l_{tse}. The storage level has lower and upper bounds L^{min} and L^{max}, respectively. Constraint (25) sets the reservoir's initial storage level to L^{init}. The inter-temporal effect of discharging water on the storage level is defined by constraint (26). The change in water level is the result of discharging water f_{tse}, spill from the reservoir f^{spill}_{tse}, and inflow F^{in}_t, which is an exogenous parameter.

F. CCGT Generation

The CCGT generator constraints are adapted from [17] and [18]. The operation of the CCGT is modelled as follows:

$$u^C_{tse} = u^C_{t-1,se} + u^{C,start}_{tse} - u^{C,stop}_{tse} \quad \forall t \in \mathcal{T}, s \in \mathcal{S}, e \in \mathcal{E} \tag{27}$$
$$u^C_{tse} \geq u^{C,start}_{tse} \quad \forall t \in \mathcal{T}, s \in \mathcal{S}, e \in \mathcal{E} \tag{28}$$
$$u^C_{tse} \leq 1 - u^{C,stop}_{tse} \quad \forall t \in \mathcal{T}, s \in \mathcal{S}, e \in \mathcal{E} \tag{29}$$
$$u^C_0 = U^C_{init} \tag{30}$$
$$u^{C,start}_{tse} \leq u^C_{t'se} \quad \forall t \in \mathcal{T}, t \leq t' \leq \min\{t + U^C_{on}, T\}, s \in \mathcal{S}, e \in \mathcal{E} \tag{31}$$
$$(1 - u^{C,stop}_{tse}) \geq u^C_{t'se} \quad \forall t \in \mathcal{T}, t \leq t' \leq \min\{t + U^C_{off}, T\}, s \in \mathcal{S}, e \in \mathcal{E} \tag{32}$$
$$g^C_{tse} + r^C_{tse} dt \leq u^C_{tse} C^c dt \qquad \forall t \in \mathcal{T}, s \in \mathcal{S}, e \in \mathcal{E} \tag{33}$$
$$u^C_{tse} C^C G^{min} dt \leq g^C_{tse} \quad \forall t \in \mathcal{T}, s \in \mathcal{S}, e \in \mathcal{E} \tag{34}$$
$$g^C_{tse} - g^C_{t-1,se} \geq -AC^C dt - u^{C,stop}_{tse}(G^{min} - A)C^C dt \quad \forall t \in \mathcal{T}, s \in \mathcal{S}, e \in \mathcal{E} \tag{35}$$
$$g^C_{tse} - g^C_{t-1,se} \leq AC^C dt + u^{C,start}_{tse}(G^{min} - A)C^C dt$$

$$\forall t \in \mathcal{T}, s \in \mathcal{S}, e \in \mathcal{E}. \tag{36}$$

$$g_0^C = G^{init} \tag{37}$$

Constraints (27)–(29) capture the state change when the CCGT is turned on or off and restrict it to be either on or off at each time $t \in \mathcal{T}$ in each scenario $(s, e) \in (\mathcal{S}, \mathcal{E})$. Constraint (30) sets the initial status of the generator to $U_{init}^C \in \{0, 1\}$. Constraints (31) and (32) ensure that the CCGT generator's operating schedule abides by its minimum up and down times which are U_{on}^C and U_{off}^C time periods, respectively; T denotes the number of time steps. Constraint (33) enforces that the CCGT generation and reserve commitments cannot exceed its installed capacity. Constraint (34) ensures that if the generator is on, it does not run below its stable load. The minimum stable load is stated as a fraction of installed capacity, such that $G^{min} \in [0, 1]$. Note that the reserve commitment is not accounted for in this constraint due to the assumption that the reserve will not be activated. Constraints (35) and (36) capture the CCGT's ramping limits. Ramping the generator is limited by a factor $A \in [0, 1]$ that represents the fraction of the capacity that can be modulated within one hour. Constraint (37) enforces the initial level of generation, G^{init}, of the CCGT.

G. Wind Power Production Modelling

Wind generation is modelled according to [16]. In the model, wind generation is defined as:

$$g_{tse\omega}^w \leq W_{tse\omega} C^W dt \qquad \forall t \in \mathcal{T}, s \in \mathcal{S}, e \in \mathcal{E}, \omega \in \Omega, \tag{38}$$

where the wind factors $W_{tse\omega} \in [0, 1]$ capture the exogenous uncertainty related to wind availability.